

MECHANICAL ALLOYING OF FeCoCr

Gema González^{1, 3*}, Dariusz Oleszak², Amaya Sagarzazu¹, Rafael Villalba¹, Lisseta D'Onofrio³

1: Laboratorio de Materiales, Departamento de Ingeniería de Materiales y Nanotecnología, Instituto Venezolano de Investigaciones Científicas, Caracas, Venezuela, 2: Faculty of Materials Science and Engineering, Warsaw University of Technology Woloska 141, 02-507 Warsaw, Poland, 3: Escuela de Física, Facultad de Ciencias, Universidad Central de Venezuela. Caracas, Venezuela

* E-mail: gemagonz@ivic.gob.ve

Recibido: 12-Nov-2009; Revisado: 27-Jul-2010; Aceptado: 04-Ago-2010

Publicado On-Line el 15-Nov-2010

Disponible en: www.rlmm.org

Abstract

The mechanical alloying of Fe-Co-Cr has been studied from the structural point of view by different techniques: XRD, TEM and Mössbauer spectroscopy, following the transformations taking place during milling. The alloys FeCo, Fe₄₀Co₅₀Cr₁₀ and Fe₅₀Co₄₀Cr₁₀ were prepared by milling of the elemental powders during 1, 2, 5, 10, 20, 40 and 60 h. The kinetics of alloy formation occurs by incorporation of Co and/or Cr in the Fe structure. For the Fe-Co alloy after 10h of milling a mixture of Fe (Co) solid solution and α -Fe is obtained. For the FeCoCr alloys prolonged milling results in Cr incorporation in the FeCo structure and a mixture of Fe (Co) and Fe (Cr) is formed. A grain size in the range of 2-5 nm is reached after 60h of milling.

Keywords: FeCo, FeCoCr, nanostructured materials, mechanical alloying

Resumen

El proceso de aleación mecánica de Fe-Co-Cr ha sido estudiado desde el punto de vista estructural por varias técnicas: DRX, MET, Espectroscopía Mössbauer, siguiendo las transformaciones que tienen lugar durante la molienda. Las aleaciones FeCo, Fe₄₀Co₅₀Cr₁₀ y Fe₅₀Co₄₀Cr₁₀ fueron preparadas a partir de los polvos elementales por molienda durante 1, 2, 5, 10, 20, 40 y 60 h. La cinética de formación de aleación ocurre por incorporación del Co y/o Cr en la estructura del Fe. Para la aleación Fe-Co después de 10 h de molienda se obtiene la mezcla de una solución sólida Fe (Co) y α -Fe. Para las aleaciones FeCoCr, la molienda prolongada resulta en la incorporación de Cr en la estructura de FeCo formándose una mezcla de Fe (Co) y Fe (Cr). Un tamaño de grano en el orden de 2-5 nm es obtenido después de 60 h de molienda.

Palabras Claves: FeCo, FeCoCr, materials nanoestructurados, aleación mecánica

1. INTRODUCTION

Mechanical alloying is able to produce nanostructure materials with unique chemical, structural, electrical and magnetic properties, due to type of disorder created by the high density of defects and the small crystal size.

The Fe-Co system is of particular interest due to its excellent magnetic properties among the Fe-alloys [1, 2]. Co forms a continuous range of solid solution with Fe all of which are ferromagnetic. Fe-50%Co has very high saturation magnetization and low magnetocrystalline anisotropy and low resistivity. The addition of Cr to Fe affects the transition temperatures from α -bcc solid solution to γ -fcc solid solution ($T_{\alpha/\alpha+\gamma}$ $T_{\alpha+\gamma/\alpha}$), increases the resistivity and improve their dynamic properties slightly

decreasing the saturation magnetization by dilution of the magnetic atoms [1], also it improves the corrosion resistance. It has been reported [3] that the addition of Cr to FeCo thin films is essential to improve magneto crystalline anisotropy in order to be use as magnetic recording material. Although several works have been reported in the Fe-Co system obtained by mechanical alloying [4-8], no reports in the Fe-Co-Cr system obtained by mechanical alloying has been found in the literature, as far as the authors know. In the present work the Fe₅₀Co₄₀Cr₁₀, Fe₄₀Co₅₀Cr₁₀ and Fe₅₀Co₅₀ systems obtained by mechanical alloying have been prepared to study the effect of the incorporation of Cr in the Fe-Co structure.

2. EXPERIMENTAL

Powders of Fe, Co and Cr (ABCR Germany) with a purity of 99.8% and particle size below 50 μm were used. The powders were mixed to give the final compositions (at.%) $\text{Fe}_{50}\text{Co}_{50}$, $\text{Fe}_{40}\text{Co}_{50}\text{Cr}_{10}$ and $\text{Fe}_{50}\text{Co}_{40}\text{Cr}_{10}$. Fritsch P5 planetary ball mill, equipped with hardened steel vials and balls (10 mm of diameter), was employed for milling with a rotational speed of 250 rpm. 10 g of powder was used and a ball-to-powder weight ratio (BPR) of 10:1. The milling periods were from 1 to 60 h. The milling experiments and all powder handling were performed under protective atmosphere of argon. Small amounts of powders were withdrawn after selected milling times for structural examinations. X-ray diffraction (XRD) was performed on a Siemens 5005 X-ray diffractometer, using $\text{Cu-K}\alpha$ (Ni filter) operating at 40 keV and 20 mA. The powder morphology as a function of milling time was studied by scanning electron microscopy (SEM) and elemental analysis was carried out by Energy Dispersive Spectroscopy (EDS). High resolution transmission electron microscopy was performed in a Philips Field emission Tecnai G2 equipment. The Mössbauer spectra were obtained with a spectrometer running in the triangular symmetric mode for velocity using a driving unit and multichannel analyzer from Wissel Ins., and a ^{57}Co in a Rh matrix. The experimental data were fitted with a Gaussian distribution, which is suitable for disordered solid solutions, since it takes into account the fact that an atom of iron is surrounded by a random number of Co(Cr) atoms. The fitting parameters are: the isomer shift with respect to metallic iron (IS), the electrical quadrupole splitting (QS), the hyperfine magnetic field (HF), the halfwidth of the gaussian distribution (Δ) and the relative subspectral area (RA). Grain size was calculated from the X-ray diffraction data applying the Scherrer equation, and the Williamson-Hall method was used to calculate grain size and strain with milling time.

3. RESULTS AND DISCUSSION

Fig. 1 shows the XRD patterns for the different alloys milled for different periods, for all the alloys the peaks broaden with milling time, suggesting a decrease in the grain size. For the Fe-Co system a slight shifting of the Fe main reflexion towards higher angles can be observed with the incorporation of Co up to 60 h of milling, this could be due to the high density of defects created during milling generating

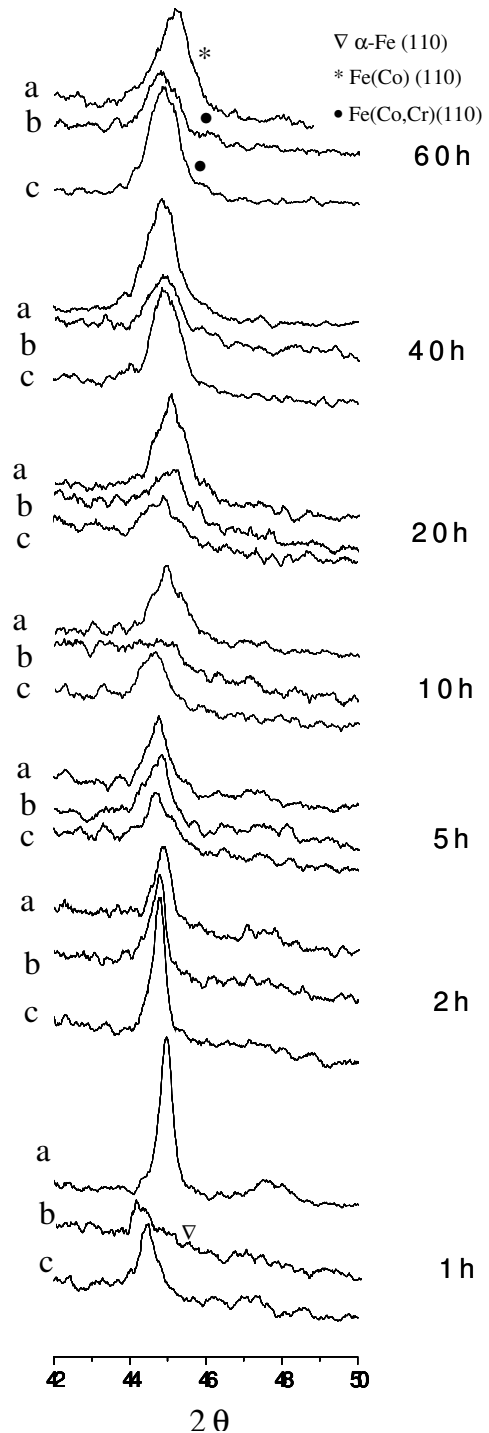


Fig. 1: XRD patterns for different milling times. a. $\text{Fe}_{50}\text{Co}_{50}$, b. $\text{Fe}_{40}\text{Co}_{50}\text{Cr}_{10}$ c. $\text{Fe}_{50}\text{Co}_{40}\text{Cr}_{10}$

a large lattice distortion. The incorporation of Cr into the structure seems to be slower than for Co, after 1 h of milling the main reflexion peak (110) is nearer to the value of Fe (110). However with increasing milling time a shift of this peak towards

higher angles is observed, indicating that the replacement of Cr by Fe causes a decrease in the lattice parameter.

Fig. 2 shows the SEM images and the EDS elemental analysis of the different alloys after 60 h of milling time. The particle agglomerates are observed after this period with smaller particle size for the Fe₅₀Co₅₀ than for the ternary alloys.

The EDS analysis show a composition almost equiatomic for the Fe₅₀Co₅₀ and a small amount of oxygen present. For the ternary compounds the atomic composition is very near to the expected from the initial mixture, this is Fe40%at, Co51%at and Cr9%at, for the Fe₄₀-Co₅₀-Cr₁₀ and Fe49.2%at, Co42.4%at and Cr 8.4 %at, for the Fe₅₀-Co₄₀-Cr₁₀. No evidence of oxygen was found in these alloys. Therefore, it can be concluded that contamination from vials and balls can be neglected. The variation of lattice parameter vs. milling time is shown in Figs. 3 for all the alloys studied. The Fe₅₀Co₅₀ shows an increase in lattice parameter up to 5 h of milling, probably due to the strong plastic deformation during milling and that the alloy is not yet completely formed. Then a progressive decrease in lattice parameter is observed with milling time reaching a value of 2.832 Å after 60h of milling, attributed to the incorporation of Co in the Fe structure. Moumeni *et al.* [8] has shown that the lattice parameter of Fe (Co) solid solution decreases as the Co content increases in samples milled for 24h.

For the Fe₅₀-Co₄₀-Cr₁₀ the lattice parameter decreases from a value near to 2.863 Å to 2.852 Å, after 20 h of milling and remains constant up to 60 h and for the Fe₄₀-Co₅₀-Cr₁₀ alloy after 2 h of milling the lattice parameter value is 2.862 Å and progressively decreases with milling time to 2.837 Å after 20 h, and then increases to 2.86 Å after 60 h of milling, probably due to an increase in the degree of order with prolonged milling. The lattice parameter of Fe decreases when Cr is added, for (Fe, Cr) solid solutions is 2.859 Å, reported in the ICDD diffraction data (JCPDS #41-1466).

The deformation versus milling time determined using the Williamson-Hall method for all the alloys is shown in Fig. 4. The Fe₅₀Co₅₀ shows a rapid increase in deformation up to 5h and then it becomes constant up to 40h, after this period a slight decrease in deformation is observed up to 60h. This may be due to lattice strain relaxation with milling time for prolonged milling.

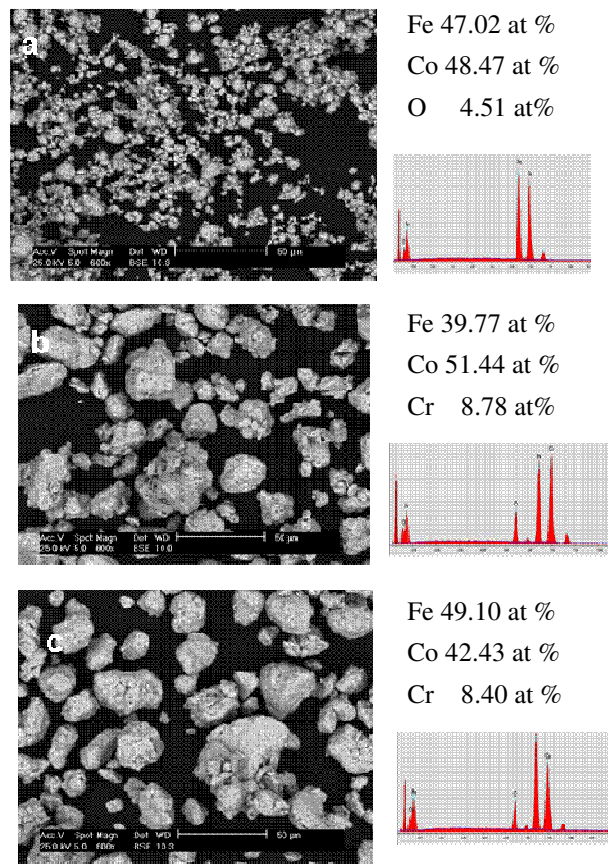


Fig. 2 SEM images and EDS analysis of alloys milled for 60 h, bar 50 µm a. Fe₅₀-Co₅₀, b. Fe₄₀-Co₅₀-Cr₁₀ c. Fe₅₀-Co₄₀-Cr₁₀

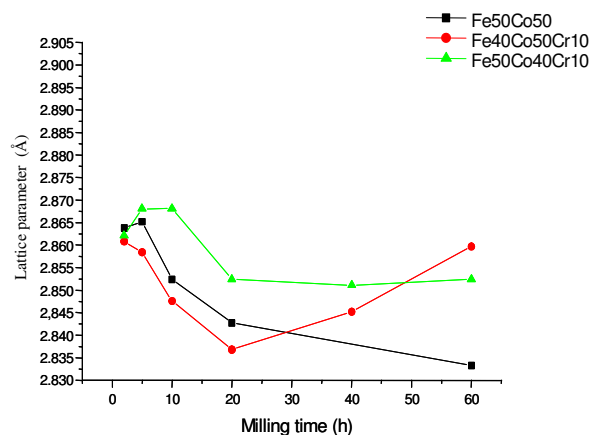


Fig. 3 Lattice parameter vs. milling time for Fe₅₀Co₅₀ and Fe-Co-Cr alloys

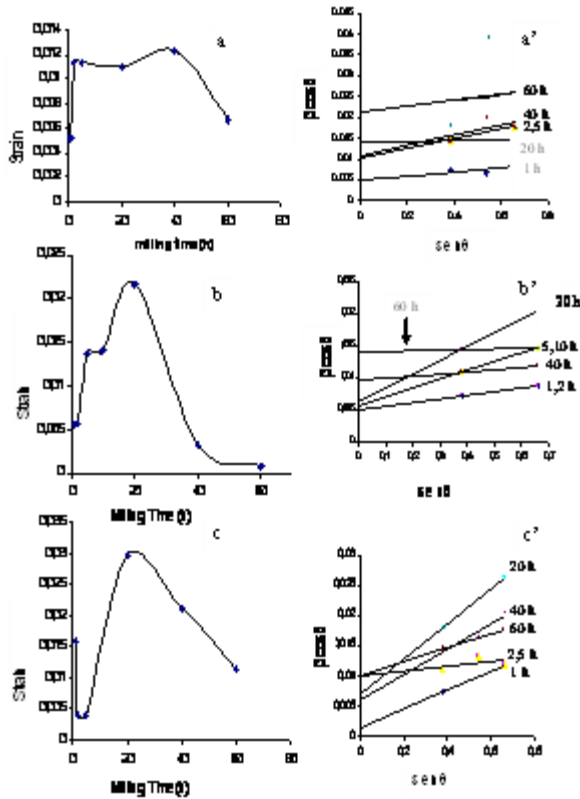


Fig.4: Lattice Strain vs milling time (a',b',c', Williamson-Hall plot) (a,a') Fe₅₀Co₅₀, (b,b') Fe₅₀Co₄₀Cr₁₀, (c,c') Fe₄₀Co₅₀Cr₁₀

The Fe₅₀-Co₄₀-Cr₁₀ and Fe₄₀-Co₅₀-Cr₁₀ show an increase in deformation up to approximately 20 h and after this period a continuous decrease is observed up to 60h. The lattice parameters for these two alloys reached the lowest value for 20 h of milling, when maximum strain was observed. The decrease in the lattice parameter may be due to the allotropic transformation, of hcp Co to fcc Co, induced by deformation. This suggests that up to this period these alloys are in the formation process.

The increase in deformation with milling time up to a maximum, for the different alloys, could be due to hardening of the materials with milling. However, the softening of the materials observed with prolonged milling can be attributed to the rearrangement of dislocation networks due to recovery of the material with the increase in temperature due to the milling process. The Scherrer equation was used to calculate grain size and the Williamson-Hall (W-H) method was used to calculate grain size and lattice strain [9]. The grain size vs. milling time for the different alloys studied is shown in Fig. 5.

A rapid decrease in grain size with milling time is

observed for all the alloys. For the Fe₅₀Co₅₀ (Fig.5a) after 5h of milling the grain size decreased to 15 nm and to 7 nm after 60h of milling. For the Fe₅₀-Co₄₀-Cr₁₀ the values calculated by W-H show a continuous decrease in grain size with milling time down to 10 nm after 60 h.

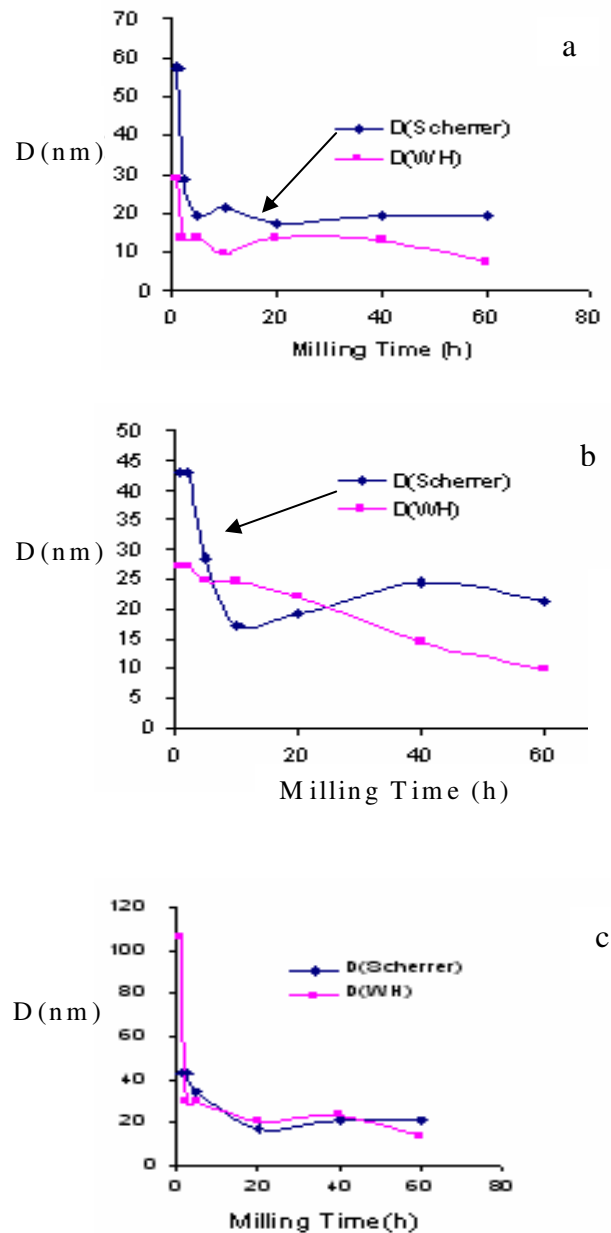


Fig. 5: Grain size vs. Milling time, calculated using Scherrer equation and by Williamson-Hall method a. Fe₅₀Co₅₀, b. Fe₅₀-Co₄₀-Cr₁₀, c. Fe₄₀-Co₅₀-Cr₁₀

For the Fe₄₀-Co₅₀-Cr₁₀ a continuous decrease in

grain size with milling time up to 20 h is observed, reaching a value of 18 nm that remains constant with prolonged milling.

The smallest grain size observed in FeCo alloys after 60 h of milling compared to the grain size in ternary alloys after the same period of milling is probably due the higher strain obtained in the binary alloys after this period.

Transmission electron microscopy confirms the decrease in grain size with milling time. All alloys reached a grain size in the range of 10-20 nm after 5h and 2- 8 nm after 60 h of milling (Fig 6). The increase in the density of defects is evident for longer milling periods; Fig. 6c, e and f show the HRTEM images after 60 h of milling, a high density of defects, twins and areas with short range order are present. Also, very small grains from 1-2 nm can be observed.

The alloys milled 60 h show a disordered region around the grains boundaries, especially evident in the $\text{Fe}_{50}\text{Co}_{50}$, this would explain the decrease in deformation observed for prolonged periods. The Mössbauer spectra at 300°K for the different alloys with milling periods of 1, 10 and 60h are shown in Fig. 7. The fitting parameters of the spectra are given in table 1. After 1 h of milling all the alloys show a HF value of 33 T corresponding to Fe. The spectra for the Fe-Co system, after 10h (Fig. 7a), show the characteristic sextet with broaden lines; two subspectra were used for the fitting process, one assigned to Fe (33 T) and the other with a HF of 34.5T assigned to Fe sites preferentially surrounded by Co atoms in the first coordination spheres, forming a disordered FeCo solid solution. DeMayo *et al.* [10] measured the variation of the hyperfine magnetic field in FeCo alloys with the composition and ordering, these authors found that the value of the hyperfine magnetic field is lower for the ordered compound than for the disordered one, the values obtained for the ordered $\text{Fe}_{50}\text{Co}_{50}$ was 33.8 T and 34.8 T for the disordered one.

After milling for 60 h, also two subspectra were used for the fitting, a magnetic one with values of the hyperfine magnetic field of 34.5 T assigned to disordered $\text{Fe}_{50}\text{Co}_{50}$ and a small paramagnetic component, probably associated to an oxide. Moumeni *et al.* [11] followed the formation of FeCo solid solution using mechanical alloying, by the evolution of the hyperfine field distribution as a function of milling time. They reported a Gaussian curve center in 35 T

after 24h of milling, related to the formation of bcc FeCo disordered solid solution.

For the Fe-Co-Cr alloys the values of the hyperfine magnetic field for the different milling periods are very similar. The spectra for 10 h of milling were fitted with two subspectra, one corresponding to Fe (33T) and other with a hyperfine magnetic field value of 34.5 T for $\text{Fe}_{50}\text{-Co}_{40}\text{-Cr}_{10}$, and a slightly lower field, 34.3 T for $\text{Fe}_{40}\text{-Co}_{50}\text{-Cr}_{10}$, due to the lower Fe content and assigned to a disordered solid solution of Fe(Co).

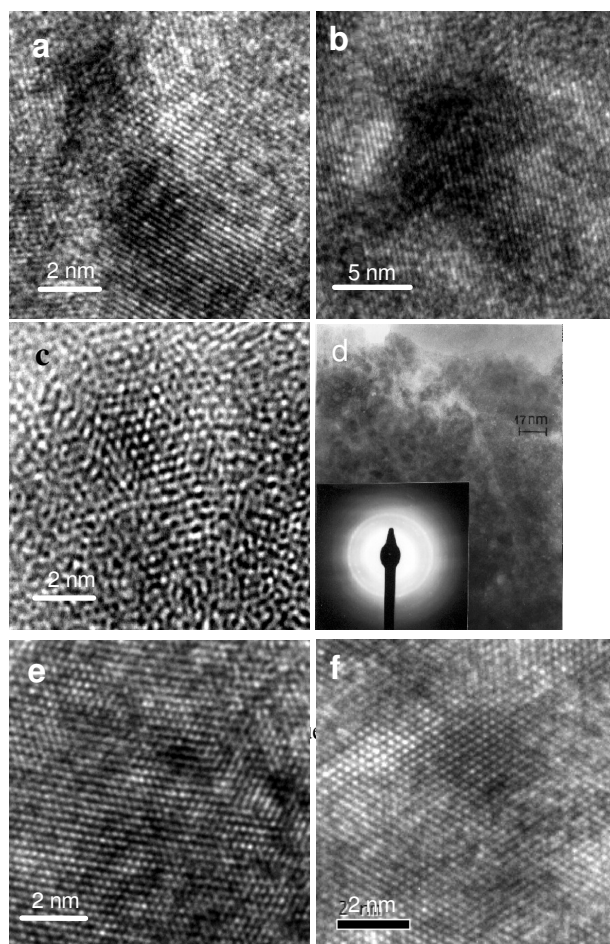


Fig. 6: TEM images a. $\text{Fe}_{50}\text{Co}_{50}$ -5h, b. $\text{Fe}_{50}\text{Co}_{40}\text{Cr}_{10}$ 5h, c. $\text{Fe}_{50}\text{Co}_{50}$ -60h, d. $\text{Fe}_{50}\text{Co}_{50}$ -60h e. $\text{Fe}_{50}\text{Co}_{40}\text{Cr}_{10}$ -60h

After 60 h of milling the characteristic sextet with broaden lines, due to the high disorder present in the alloys, is observed. Two subspectra were used in the fitting, one component having a field of 30.3 T assigned to the solid solution Fe(Cr) and the second component having a hyperfine magnetic field value

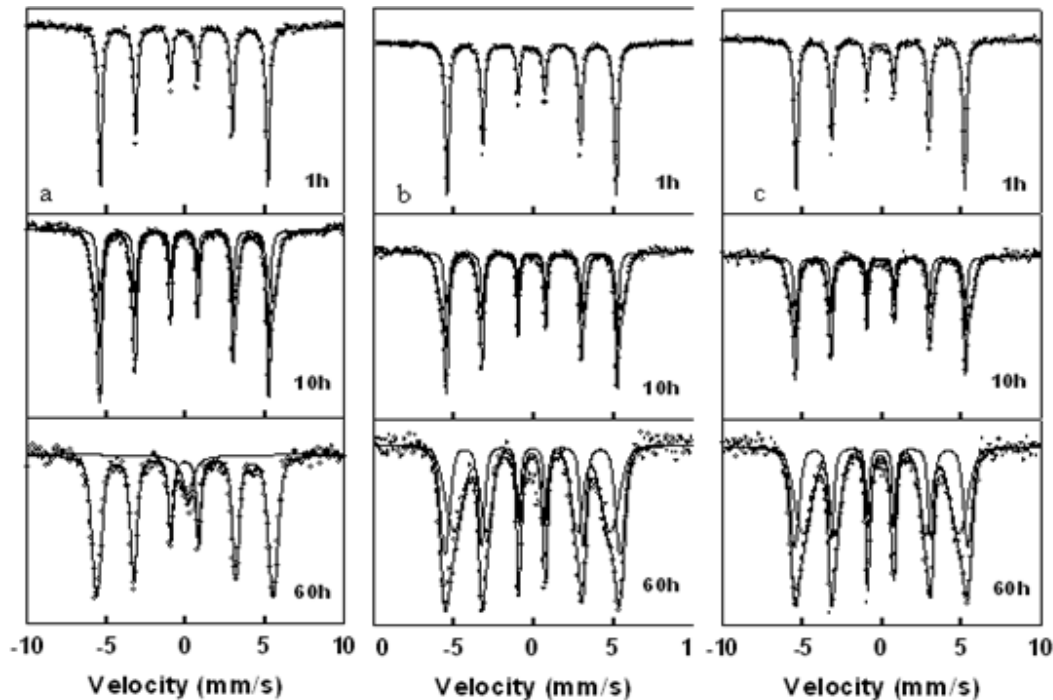


Fig.7: Mössbauer spectra of alloy for different milling periods (a) $\text{Fe}_{50}\text{Co}_{50}$ (b) $\text{Fe}_{50}\text{Co}_{40}\text{Cr}_{10}$ (c) $\text{Fe}_{40}\text{Co}_{50}\text{Cr}_{10}$

Table 1: Mössbauer parameters

Sample	MA	IS	QS	HF	Δ	RA
	time (h)	(mm/s)	(mm/s)	T	T	%
$\text{Fe}_{50}\text{Co}_{50}$	1	0.00	0.00	33	NA	100
	10	0.00	0.00	33	3.0	41
		0.03	0.00	34.5	1.8	59
	60	0.04	0.00	34.5	1.4	91
0.22		0.00	0.0	NA	9	
$\text{Fe}_{50}\text{Co}_{40}\text{Cr}_{10}$	1	0.00	0.00	33	NA	100
	10	0.00	0.00	33	0.2	38
		0.03	0.00	34.5	1.9	62
	60	0.00	0.00	30.3	3.1	59
0.04		0.00	34	1.5	41	
$\text{Fe}_{40}\text{Co}_{50}\text{Cr}_{10}$	1	0.00	0.00	33	NA	100
	10	0.00	0.00	33	0.2	36
		0.03	0.00	34.3	1.9	64
	60	0.00	0.00	30.3	3.0	62
0.04		0.00	33.7	1.3	38	

IS: isomeric shift, QS: electrical quadrupole splitting, HF: hyperfine magnetic field, Δ : Halfwidth of the Gaussian fitting, RA: relative subspectral area, N.A.= not applicable

of 34.0 T for $\text{Fe}_{50}\text{Co}_{40}\text{Cr}_{10}$ and 33.7 T for the $\text{Fe}_{40}\text{Co}_{50}\text{Cr}_{10}$, assigned to Fe(Co) disordered solid solution. The small decrease of the HF value

observed in the second component with respect of that of FeCo (34 and 33.7 instead of 34.5) may be related to an increased degree of order in these alloys. It can be observed that Cr decreases the value of the Fe hyperfine magnetic field as has been reported elsewhere [12].

The relative areas of both phases, after this milling time, are $\cong 40\%$ Fe(Co) and 60% Fe(Cr), the increase in the relative area is observed with milling time, indicating that diffusion of Cr in Fe is slightly higher in the alloy with lower Fe content. A detailed discussion of the Mössbauer results has been published by D'Onofrio *et al* [13].

4. CONCLUSIONS

For the Fe-Co system a mixture of Fe(Co) solid solution and α -Fe is formed after 10h of milling, for FeCoCr alloys a mixture of Fe(Co) and Fe(Cr) solid solutions is obtained for this period. After prolonged milling Cr incorporates in the FeCo structure and a mixture of Fe(Cr) and FeCoCr solid solutions is obtained. All the alloys reached a uniform nanograin size in the range of 2-5 nm after 60 h of milling, with high density of defects. The addition of Cr decreases the hyperfine magnetic field of FeCo. A maximum lattice deformation is reached after 20 h of milling for the alloys with Cr additions and then a decrease, probably due to strain release with prolonged milling time.

The hyperfine magnetic field parameters for both Fe₄₀Co₅₀Cr₁₀ and Fe₅₀Co₄₀Cr₁₀ alloys were very similar, however higher Cr diffusion into the Fe(Co) structure is observed for the alloy with lower Fe content.

5. REFERENCES

- [1] Couderchon C and Tiers JF. *J. Mag.and Mag. Mat* 1982; **26**: 196-214.
- [2] Vincze I, Campbell IA, Meyer AJ. *Sol. State. Comm* 1974; **15** (9): 1495-1499.
- [3] Bozorth RM, *Ferromagnetism*, IEEE, (NY): 1991.
- [4] Kuhrt Ch, Schultz L. *J. Appl. Phys.* 1992; **71**(4): 1896-1900.
- [5] Collins GS and Meeves BH. *Script. Metall. Mat.* 1993; **29**: 1319-1323.
- [6] Kim YD, Chung JY, Kim J, Jeon H. *Mat. Sci. Eng.* 2000; **A291**: 17-21.
- [7] Gonzalez G, Sagarzazu A, Villalba R, Ochoa J, D'Onofrio L. *Mat. Sci. Forum* 2001; **360-362**: 355-360.
- [8] Moumeni H, Alleg S, Djebbari C, Bentayeb FZ, *J. Mat. Sci.* 2004; **39**: 5441-5443.
- [9] Williamson GK, Hall WH, *Acta Metall.* 1953; **1**:22-31.
- [10] DeMayo B, Forester DW, Spooner S. *J.Appl. Phys.* 1970; **41** (3):1319-1320.
- [11] Moumeni H, Alleg S, Greneche JM. *J. Alloys and Compounds* 2005; **386**:12-19.
- [12] Fnidiki A, Lemoine C, Teillet J. *Physica* 2005; **B357**: 319-325.
- [13] D'Onofrio L, Gonzalez G, Oleszak D, Sagarzazu A, Villalba R. *Hyperfine Interactions*, 2010 ; **195**(1-3) :167-171.